[CANCER RESEARCH 60, 2258–2262, April 15, 2000]

Dihydrotestosterone as a Selective Cellular/Nuclear Localization Vector for Anti-Gene Peptide Nucleic Acid in Prostatic Carcinoma Cells[1]

Lidia C. Boffa[2], Sonia Scarfi', Maria Rita Mariani, Gianluca Damonte, Vincent G. Allfrey, Umberto Benatti, and Patricia L. Morris

National Cancer Institute, IST, 16132 Genoa, Italy [L. C. B., M. R. M.]; Department of Experimental Medicine, Biochemistry Section, University of Genoa, 16132 Genoa, Italy [S. S., G. D., U. B.]; The Rockefeller University, 1230 York Avenue, New York, New York 10021 [V. G. A., P. L. M.]; and Population Council, 1230 York Avenue, New York, New York 10021 [P. L. M.]

ABSTRACT

Peptide nucleic acids (PNAs) are synthetic structural analogues of DNA and RNA that, if allowed to enter the cell, bind to the complementary polynucleotide sequence and inhibit DNA transcription and mRNA translation. Although PNAs have a very limited ability in penetrating nuclei of living cells, there are indications that covalent linkage of the PNA to appropriate vectors, *e.g.*, a nuclear localization signal, permits access to the genome. Here we test the ability of dihydrotestosterone (T) covalently linked to PNA to act as a vector for targeting c-*myc* DNA to prostatic cancer cell nuclei. LNCaP cells, which express the androgen receptor gene, and DU145 cells, in which the androgen receptor gene is silent, offer a model to test this biologically active hormone as a cell-specific vector. T vector was covalently linked to the NH_2-terminal position of a PNA complementary to a unique sequence of c-*myc* oncogene (PNAmyc-T). To localize PNAmyc-T and vector-free PNA within the cells, a rhodamine (R) group was attached at the COOH-terminal position (PNAmyc-R, PNAmyc-TR); cellular uptake was monitored by confocal fluorescence microscopy. PNAmyc-R was detected only in the cytoplasm of both prostatic cell lines, whereas PNAmyc-TR was localized in nuclei as well as in cytoplasm of LNCaP cells. In contrast, PNAmyc-TR uptake in DU145 cells was minimal and exclusively cytoplasmic. In LNCaP cells, MYC protein remained unchanged by exposure to vector-free PNAmyc, whereas a significant and persistent decrease was induced by PNAmyc-T. In DU145 cells, MYC expression was unaltered by PNAmyc with or without the T vector. Our data show that the T vector facilitates cell-selective nuclear localization of PNA and its consequent inhibition of c-*myc* expression. These findings suggest a strategy for targeting of cell-specific anti-gene therapy in prostatic carcinoma.

INTRODUCTION

PNAs[3] are synthetic structural homologues of nucleic acids in which the negatively charged phosphate-sugar backbone of the polynucleotide is replaced by an uncharged polyamide backbone consisting of achiral *N*-(2-aminoethyl) glycine units. Each unit is linked to a purine or pyrimidine base to create the specific sequence required for hybridization to the targeted polynucleotide (1, 2). There are numerous advantages of PNA in anti-gene or antisense applications to down-regulate transcription or translation in living cells. The absence of a negatively charged backbone facilitates PNA invasion of the DNA double helix to form a stable PNA-DNA hybrid with high mismatch discrimination (3, 4). This interaction is further stabilized in chromatin of live cells by two important observations: it has been demonstrated that in the cellular environment, PNA-DNA hybrids are more stable than their homologues DNA-DNA because they are ionic strength independent (5); and PNA binding to supercoiled DNA is stronger than to linear DNA and favored in transcriptionally active chromatin (6, 7). The great stability of PNA-DNA hybrids in chromatin has made it possible to isolate the hybrids as components of restriction fragments as large as 23 kb (8). Moreover, the unusual chemical structure of PNAs makes them highly resistant to both nucleases and proteases (9).

Previous experiments with permeabilized cells, isolated nuclei (10, 7), and also *in vivo* (11) have shown that complex sequence PNAs are highly effective in blocking transcription of the targeted gene without inhibiting RNA synthesis in unrelated genes. It has also been shown that PNA binding effectively blocks transcription of the c-*myc* gene in both directions (7). Still, a major problem in the application of PNAs as anti-gene agents is their restricted ability to penetrate the nucleus of a cell in culture or *in vivo* (11, 12). However, there are indications that antisense or anti-gene PNAs, if artificially allowed to enter the nucleus, can inhibit translation/transcription (7, 10, 13). Recent trials of a few vectors have also shown a successful delivery of the fused PNAs to the nucleus of live cells (11, 14–17).

Nevertheless, a PNA targeting specificity within cell lines of identical origin but differing by a crucial single cell function has not been demonstrated to date.

Here we examine the possibility of using the biologically active form of testosterone, T, as a cell-specific PNA vector to target the c-*myc* gene in prostatic carcinoma cells. Two cell lines were selected: LNCaP, which expresses the AR gene, and DU145, in which the AR gene is silent (18, 19). T was covalently linked to the NH_2-terminal position of an anti-gene PNA that specifically targets a unique sequence in the second exon of c-*myc* ($PNAmyc_{wt}$-T), a gene that, in these cell lines, regulates growth and proliferation (20). We confirm that the c-*myc*-targeting PNA, when covalently linked to the vector, can enter the nucleus of living LNCaP cells and inhibit MYC expression. These findings suggest a strategy for the cell-specific targeting of anti-gene therapy.

MATERIALS AND METHODS

PNA Design. We have used the set of nine related PNA constructs shown in Table 1 to study the role of the T vector in directing their intracellular localization and their effects on c-*myc* expression. $PNAmyc_{wt}$ represents a unique sequence of c-*myc* (accession no. X00364; Ref. 21) located in the second exon of the oncogene (base 4528–4544; TCAACGTTAGCTTCACC). This sequence was tested with and without the T vector, which was covalently linked in the NH_2-terminal position ($PNAmyc_{wt}$-T; Table 1). In the first set of experiments, these two PNAs were tagged at their COOH-terminal end with R to allow their localization within the cell by fluorescence/phase contrast confocal microscopy (Table 1).

A R tag was also used to test the specificity of a PNA construct (PNA-myc_{mut}-R) containing a three bases substitution in the c-*myc* sequence, thus leaving the purine:pyrimidine ratio unchanged (TTAACGCTAGCTT-TACC). Other constructs containing this mutant sequence also served as negative controls (Table 1).

As a positive control, we also tested the wild-type PNAmyc sequence

Received 11/8/99; accepted 2/16/00.

The costs of publication of this article were defrayed in part by the payment of page charges. This article must therefore be hereby marked *advertisement* in accordance with 18 U.S.C. Section 1734 solely to indicate this fact.

[1] Supported by Associazione Italiana per la Ricerca sul Cancro; Target Projects "Biotechnology" Consiglio Nazionale delle Ricerche; Consiglio Nazionale delle Ricerche/Consejo Nacional de Ciencia y Tecnologia (to L. C. B.) and "Biotechnology" Consiglio Nazionale delle Ricerche, PRIN 1999 by Ministero dell'Università e Ricerca Scientifica e Tecnologica (to U. B.); and NIH Grants HD-29428 and HD-13541 (to P. L. M.).

[2] To whom requests for reprints should be addressed, at the Department of Experimental Oncology, National Cancer Institute, IST, L.go R. Benzi 10, 16132 Genoa, Italy; Email: boffa@hp380.ist.unige.it.

[3] The abbreviations used are: PNA, peptide nucleic acid; AR, androgen receptor; Boc, tertbutoxycarbonyl; R, rhodamine; T, dihydrotestosterone; NLS, nuclear localization signal peptide; TFA, trifluoroacetic acid; HPLC, high-performance liquid chromatography.

Downloaded from http://aacrjournals.org/cancerres/article-pdf/60/8/2258/2484015/ch08000002258.pdf by guest on 06 October 2024

Table 1 *PNAs in the study*

Description	Abbreviation	COOH-terminal modification	PNA sequence	NH_2-terminal modification
c-*myc* anti-gene	PNA-myc_{wt}		TCAACGTTAGCTTCACC	
c-*myc* anti-gene rhodaminated	PNA-myc_{wt}-R	R	TCAACGTTAGCTTCACC	
c-*myc* anti-gene linked to T	PNA-myc_{wt}-T		TCAACGTTAGCTTCACC	T
c-*myc* anti-gene rhodaminated and linked to T	PNA-myc_{wt}-TR	R	TCAACGTTAGCTTCACC	T
c-*myc* anti-gene linked to a NLS	PNA-myc_{wt}-NLS		TCAACGTTAGCTTCACC	[PKKKRKV] (NLS)
c-*myc* anti-gene modified by a three-point mutation	PNA-myc_{mut}		**TT**AACG**CT**AGCTT**TA**CC	
Rhodaminated c-*myc* anti-gene, modified by a three-point mutation	PNA-myc_{mut}-R	R	**TT**AACG**CT**AGCTT**TA**CC	
c-*myc* anti-gene modified by a three-point mutation linked to T	PNA-myc_{mut}-T		**TTA**ACG**CT**AGCTT**TA**CC	T
Rhodaminated three-point mutation c-*myc* anti-gene linked to T	PNA-myc_{mut}-TR	R	**TT**AACG**CT**AGCTT**TA**CC	T

($PNAmyc_{wt}$) coupled to the SV40 NLS PKKKRKV (22), which we already showed allows the anti-gene $PNAmyc_{wt}$ to penetrate intact cell nuclei and efficiently down-regulate c-*myc* overexpression in Burkitt's lymphoma cells (23).

PNA Synthesis. All PNAs used in this work (Table 1) were manually synthesized using a standard method of solid phase peptide synthesis, which follows the Boc strategy (24, 25) with minor modifications to allow PNA rhodamination.

Briefly, 25 nmol of 4-methyl-benzhydril-amine-polystyrene-Gly-Boc deprotected resin (Novabiochem AG, Laufelfingen, Switzerland) were treated for 20 min at 40°C with a coupling reaction mixture containing 4.5 eq of *o*-(7-azabenzotriazol-1-yl)-1,1,3,3-tetramethyl-uronium hexafluorophosphate (Perseptive Biosystems, PRIMM, Milan, Italy), 5 eq of *N*,*N*-diisopropylethylamine (Fluka Chemie AG, Buchs, Switzerland), and 7.5 eq of Sim-Collidine (Fluka) with the addition of 5 eq of α-Boc-Lysine-(ϵ- fluorenylmethoxycarbonyl)-OH (Novabiochem) for rhodaminated PNAs, or alternatively 5 eq of α-Boc-Lysine-(ϵ-Z)-OH for nonrhodaminated constructs at 0.1 M final concentration in anhydrous *N*-methyl pyrrolidone (Fluka).

Once lysine was coupled to the resin, its fluorenylmethoxycarbonyl-protected ϵ amino group was selectively deprotected by a 20-min reaction with 20% piperidine (Fluka) in anhydrous dimethylformamide (Fluka). Another treatment with the above coupling mixture with the addition of 5 eq of rhodamine B (Sigma) was then performed to obtain a selective rhodamination of the lysine's ϵ amino group.

Subsequently, in the assembling of the PNA constructs, first the linker (Boc-8-amino-3, 6 dioxa-octanoyl acid; PRIMM) was added and then the Boc-PNA monomers (PRIMM) were added according to the PNA sequence. Once the synthesis of the PNA plus one linker was completed, a small portion of the product assembled on the resin was deprotected, cleaved, and purified to determine the mass spectrum. To the bulk of the PNA still linked to the resin, a second linker was added followed by 4,5-dihydrotestosterone hemisuccinate ($\geq$98% purity; Fluka). All of the reactions described were performed in the same coupling mixture after deprotection of Boc-α-amino groups following standard TFA procedure to form a pseudopeptidic bond.

PNA Characterization and Purification. All synthesized compounds were analyzed and purified by reverse phase HPLC. The analysis of each crude product was performed using a HP 1090 HPLC equipped with a Waters C_{18} μBondapack column (3.9 $\times$ 300 mm), while the purification was obtained on a Shimadzu LC-8A preparative HPLC equipped with a Waters C_{18} μBondapack column (19 $\times$ 300 mm). For both analyses, the solvent gradient program started with 100% solvent A (0.1% TFA in water) for 5 min; solvent B (0.1% TFA in acetonitrile) was then added with a linear increase up to 40% in 30 min and subsequently up to 100% solvent B in 5 min. The column eluates were monitored with a diode array detector set at 260 nm. Fractions containing the purified products were pooled, vacuum-dried, resuspended in TFA, and precipitated with ice-cold diethyl ether.

Mass spectra of each compound were determined using a single quadrupole HP Engine 5989-A equipped with an electrospray ion source (ESMS) and set in the positive ion mode.

Cell Culture. Two prostatic carcinoma-derived cell lines were used (LNCaP and DU145 cultured in RPMI 1640, 10% charcoal-stripped FCS). Their features and culture conditions were as previously detailed (26, 27). PNA stock solutions (500 μM in H_2O neutralized with NaOH) were added as an aliquot to the culture medium to their final concentration. For PNA cellular localization experiments, cells were cultured for 24 h in the presence of 2 μM $PNAmyc_{wt}$-R or $PNAmyc_{wt}$-TR, their maximal soluble concentration in rhodaminated conditions. In the gene regulation experiments, $PNAmyc_{wt}$, $PNAmyc_{wt}$-T, $PNAmyc_{mut}$-T, and $PNAmyc_{wt}$-NLS were present at a final 10-μM concentration in the culture medium for 0, 24, 48, or 72 h. Cell growth was measured by total cell counts from three replicate flasks (1.3–5.0 $\times$ 10^6/75-cm^2 flask), whereas cell viability was determined by trypan blue exclusion. The SD was calculated both for cell growth and viability keeping into account the data from all of the experiments (minimum of three each).

Cell Fixation, Staining, and Confocal Microscopy. In three identical experiments after 24-h exposure to $PNAmyc_{wt}$-R and $PNAmyc_{wt}$-TR, cells were washed and resuspended in PBS at a final concentration of 10^6 cells/ml, then fixed by the addition of an equal volume of 4% paraformaldehyde at 0°C for 20 min (28), centrifuged, and resuspended in MOWIOL (1.6 $\times$ 10^4 cells/μl; Calbiochem-Novabiochem, San Diego, CA). The cell suspension was spotted on a glass slide in two aliquots of 10 and 5 μl, covered, and sealed. Confocal microscopy was performed with a Bio-Rad MRC-1024 Confocal Laser Scanning System equipped with a Zeiss Axioskope (Bio-Rad, Microscopy Division, Hertfordshire, United Kingdom). Bio-Rad Laser Scharp Graphic was interfaced for image acquisition using COMOS Bio-Rad software. The laser filter was yellow (568 nm), and the objective magnification was $\times$100. Images were acquired in 0.36-μm layers, both in fluorescence and "phase-contrast" mode.

Western Blot Analysis. Total cellular proteins samples were derived from 10^7 cells solubilized in 200 μl of urea lysis buffer [9 M urea, 50 mM Tris (pH 7.0)] with brief sonication at 0°C as needed.

Western blot analysis for MYC expression was performed as described previously (29). Briefly, total cellular proteins were electrophoretically separated using 10% acrylamide and 0.4% (w/v) SDS gels and then transferred to a nitrocellulose membrane (Hybond C-extra, Amersham). The membrane was then cut at a 45–50-kb molecular weight level (using as reference kaleidoscope prestained standards; Bio-Rad). Both membrane halves were incubated in parallel overnight with a primary antibody [top with anti-myc antibody (9E10 Calbiochem, San Diego, CA); bottom with anti-H2b antibody kindly provided by Dr. M. Romani, IST (Genova, Italy)]. The membranes were washed and exposed to a rabbit antimouse IgG (Dakopatts, Glostrup, Denmark) at room temperature for 1 h. MYC and H2b bands were visualized by the incubation of the membrane with alkaline phosphatase-conjugated goat antirabbit IgG (Sigma) at room temperature for 2 h followed by exposure to the 5-bromo-4-chloro-3-indolylphosphate/nitro blue tetrazolium substrate developer (Sigma).

The stained and reassembled Western blot images from triplicate experiments were digitally acquired, elaborated in Photoshop, and then quantified using Scion-Image. MYC concentrations were normalized to the matching histone H2b concentrations (a protein that remains constant throughout the treatment described). Therefore, MYC concentration is reported as a ratio to an H2b standard. For Western blot analyses, the average error was 14.0% (range, 8.3–25.1%) in the LNCaP experiments, and for those with DU145, the average error was 10.2% (range, 8.5–20.3%).

RESULTS

PNA Design and Synthesis. The structure of a PNA modified at its COOH-terminal by rhodamination and at its NH_2-terminal by the addition of T vector is shown in Fig. 1. The reaction of R's carboxyl group with the amino group of the COOH-terminal lysine did not alter the fluorescence of R, thus allowing detection of PNA distribution in the cell. In the more complex constructs, the PNA component was deliberately spaced at a distance from both the T vector and the R fluorophore to assure unimpeded bp matching of the PNA anti-gene to the complementary sequence of the target c-*myc* gene. The spacing

Downloaded from http://aacrjournals.org/cancerres/article-pdf/60/8/2258/2484015/ch0800002258.pdf by guest on 06 October 2024

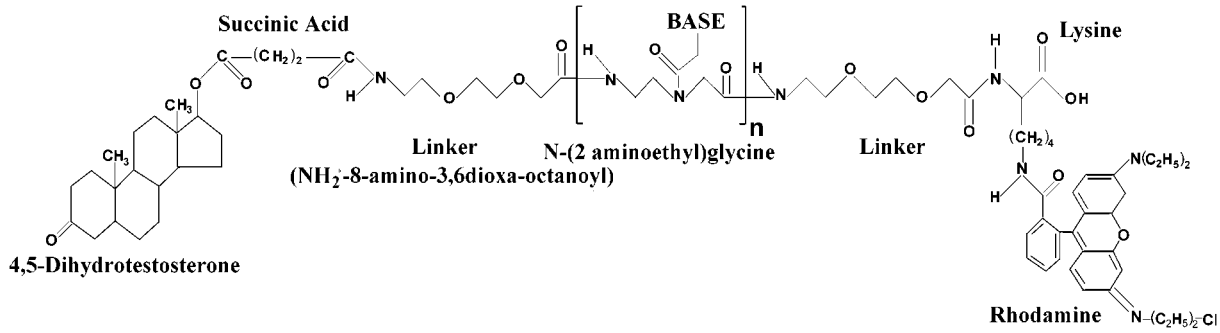

Fig. 1. Chemical structure of the PNA-TR construct.

was obtained by the addition of an octanoyl linker to the NH_2- and COOH-termini of the PNA. The hemisuccinate derivative of T was linked by its carboxyl group to the NH_2-terminal group of the PNA molecule. Furthermore, the succinic acid extension of the vector acts as an additional spacer that may give improved flexibility to the construct and enhance the steric freedom needed for T to interact with the AR in the nucleus of the target cells.

The syntheses of the PNA constructs listed in Table 1 had final yields of 40–50%. After preparative reverse phase HPLC, the purity of each product ranged between 90 and 95%. In all cases, the mass spectra of the purified PNAs showed [M+H]+ ions values consistent with the molecular weights of the expected molecules. In the specific case of the PNAs linked to T in the NH_2-terminal position, the mass spectra acquired both before and after the T coupling reaction confirmed the correct assembly of the PNA constructs.

Detailed Description of the PNA and PNA Constructs. Table 1 contains a description of the experimental PNAs used in this study, including their modifications and corresponding abbreviations. In particular, PNA-myc_{wt} is a 17-mer PNA anti-gene for the unique sequence of c-*myc*, bases 4528–4544, in its II exon (21). We noted that the addition of R to PNA and to any of its constructs resulted in a marked decrease in their solubility in the cell culture medium. The maximum solubility of PNA-myc_{wt}-R and PNA-myc_{wt}-TR in RPMI complete medium was only 2 μM; any attempt to increase it resulted in precipitation. All of the other PNAs listed in Table 1 had solubilities in excess of 500 μM (stock solution in "Materials and Methods") far above the 10 μM concentration used in most experiments.

Cell and Nuclear-specific Targeting by PNA Constructs. To test whether the covalent attachment of the T vector to PNAs allowed their binding to the AR and transport into the nuclei of intact cells, LNCaP and DU145 cells were exposed to 2 μM PNA-myc_{wt}-R and PNA-myc_{wt}-TR and cultured for 5, 10, and 24 h. Although intracellular fluorescence was already detectable after 5 h (data not shown), the maximum intensity was obtained at 24 h. Untreated cells showed only background intracellular fluorescence after 24 h (data not shown). In LNCaP cells exposed to the vector-free PNA-myc_{wt}-R, the fluorescence had a cytoplasmic localization (Fig. 2, *A* and *E*), whereas PNA-myc_{wt}-TR was also clearly detectable in the cell nuclei (Fig. 2, *B* and *F*). In DU145 cells, both PNA-myc_{wt}-R (Fig. 2, *C* and *G*) and PNA-myc_{wt}-TR (Fig. 2, *D* and *H*) fluorescence was entirely cytoplasmic. Notably, this fluorescence in DU145 cells was far weaker in the construct carrying the T vector than in the matching PNA-myc_{wt}-R. This effect was probably due to the lack of ARs in DU145 cells combined with the bulkiness and low solubility of the PNA-myc_{wt}-TR construct.

Thus, the T vector met two criteria for effective PNA delivery, namely recognition of cell phenotype and transport into the nucleus.

PNA cellular localization was also quantified, not only in the final images, but also on all of the sections of the confocal acquisitions. Differences were significant when the optical sections passing through the middle of the nuclei (23) were evaluated (data not shown).

Effects of PNAs on Cell Growth. The PNA concentration of 10 μM in the cell medium was chosen because we have previously proven that in similar experimental conditions, this PNA-myc_{wt}-NLS concentration caused maximum inhibition of MYC expression with a small decrease in cell viability (23).

In LNCaP cells, exposure to PNA-myc_{wt}-T and to PNA-myc_{wt}-NLS caused a time-dependent decrease in cell growth that became as low as 34% of the control at 72 h. Treatment with any of the other nonrhodaminated PNAs listed (Table 1), other than PNA-myc_{wt}-T and PNA-myc_{wt}-NLS, resulted in cell growth rates essentially superimposable to those of untreated cells (Fig. 3*A*).

In DU145 cells only, the construct PNA-myc_{wt}-NLS was used as a

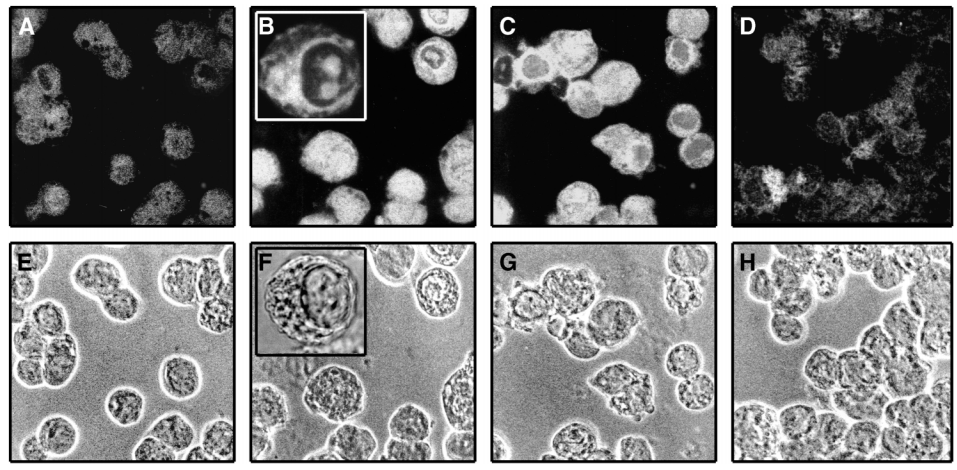

Fig. 2. Cellular localization of PNAs in LNCaP and DU145 cells. Cells were cultured in the presence of 2-μM R-tagged PNA constructs for 24 h and subsequently processed for microscopy analysis using confocal fluorescence (*A–D*) or phase-contrast microscopy (*E–H*). Panels *A* and *E* and panels *C* and *G*, show the cellular localization of PNA-myc_{wt}-R in LNCaP and DU145 cells, respectively, whereas for PNA-myc_{wt}-TR, cytoplasmic and also nuclear localization is shown in LNCaP cells (*B* and *F*) but not in DU145 cells (*D* and *H*). *Inset* (*top left corner* of *B* and *F*), at a higher magnification, the intranuclear localization of PNA-myc_{wt}-TR in LNCaP cells.

Downloaded from http://aacrjournals.org/cancerres/article-pdf/60/8/2258/2484015/ch0800002258.pdf by guest on 06 October 2024

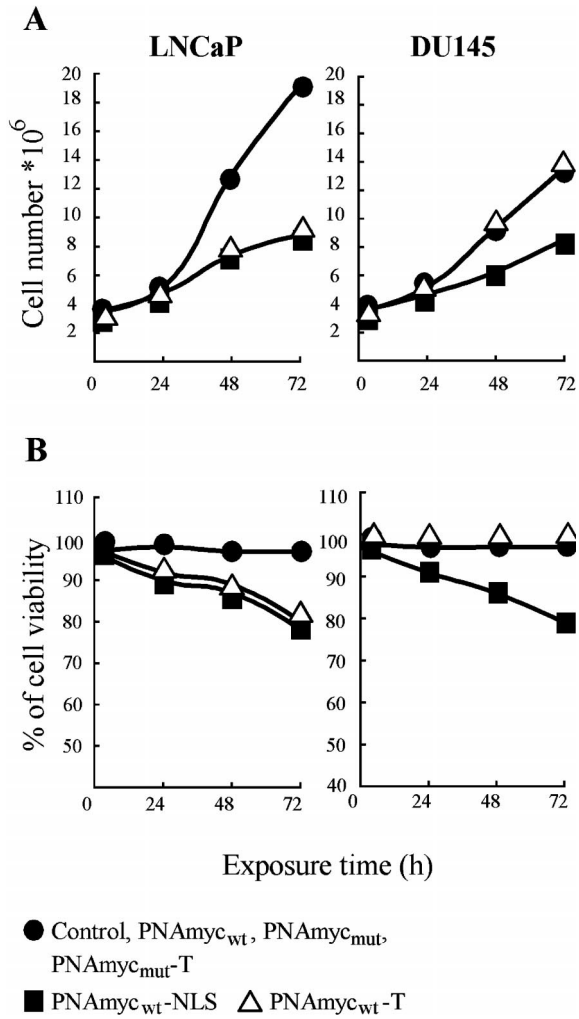

Fig. 3. Effects of PNAs on cell growth. LNCaP and DU145 cells were treated with a 10-μM concentration of PNA constructs in the culture medium [PNA-myc$_{wt}$-T (△), PNA-myc$_{wt}$, PNA-myc$_{mut}$, and PNA-myc$_{mut}$-T (●) as negative controls, and PNA-myc$_{wt}$-NLS (■) as a positive control]. Cell numbers (*A*) and viability (*B*) were estimated, as described in "Materials and Methods," at increasing times of exposure to different PNA constructs.

positive control for nuclear localization and resultant c-*myc* gene down-regulation. As we already showed, this NLS effectively delivers PNA to cells in a specific way (23), resulting in a time-dependent inhibition of cell growth of 36% at 72 h. The SD for triplicate experiment is not illustrated in the graphs because its range is only between 1.1 and 5.8% for LNCaP cells and 1.3 and 6.1% for DU145 cells.

Effects of PNAs on Cell Viability. In LNCaP cells, exposure to either PNA-myc$_{wt}$-T or PNA-myc$_{wt}$-NLS caused a modest time-dependent decline in cell viability, which reached only about 20% after 72 h of treatment. An effect on the viability of the same magnitude and timing was also observed in DU145 cells, but only when treated with PNA-myc$_{wt}$-NLS. In both cell lines, exposure to any of the (nonrhodaminated) PNAs had no effect on viability as compared to untreated cells (Fig. 3*B*). The SD is not reported graphically because it ranged only between 2 and 6% both for LNCaP and DU145 cell lines.

Modulation of c-*myc* Expression by PNAs. The effects of PNAs on expression of the c-*myc* gene in LNCaP and DU145 cells were monitored by immunochemical measurement of the MYC protein content of cell lysates using data obtained from at least a triplicate run of each set of immunostained Western blots as described in "Materials and Methods." In each case, the MYC content of the whole cell lysate was compared to that of histone H2b, a protein that remains constant throughout the treatment described. The constancy of H2b made it possible to represent variations in MYC protein concentration normalized to the H2b content in the same lysate (Fig. 4).

We compared the effects of the PNAs on MYC expression in parallel cultures of LNCaP and DU145 cells exposed to 10 μM each of the nonrhodaminated PNAs (listed in Table 1) for 0, 24, 48, or 72 h. Under these conditions, a time-dependent decrease in MYC content was observed in LNCaP cells, but only by treatment with PNAs covalently linked to vectors: PNA-myc$_{wt}$-T and PNA-myc$_{wt}$-NLS. In both cases, the decrease was time-dependent, yet different for the two vectors. Whereas PNA-myc$_{wt}$-NLS induced a linear decrease in MYC content (up to 52% at 72 h), PNA-myc$_{wt}$-T caused a maximal effect (−63%) at 24 h as compared to −50% or −42% at 48 or 72 h, respectively (Fig. 4). In DU145 cells that lack AR, only PNA-myc$_{wt}$-NLS caused a time-depen-

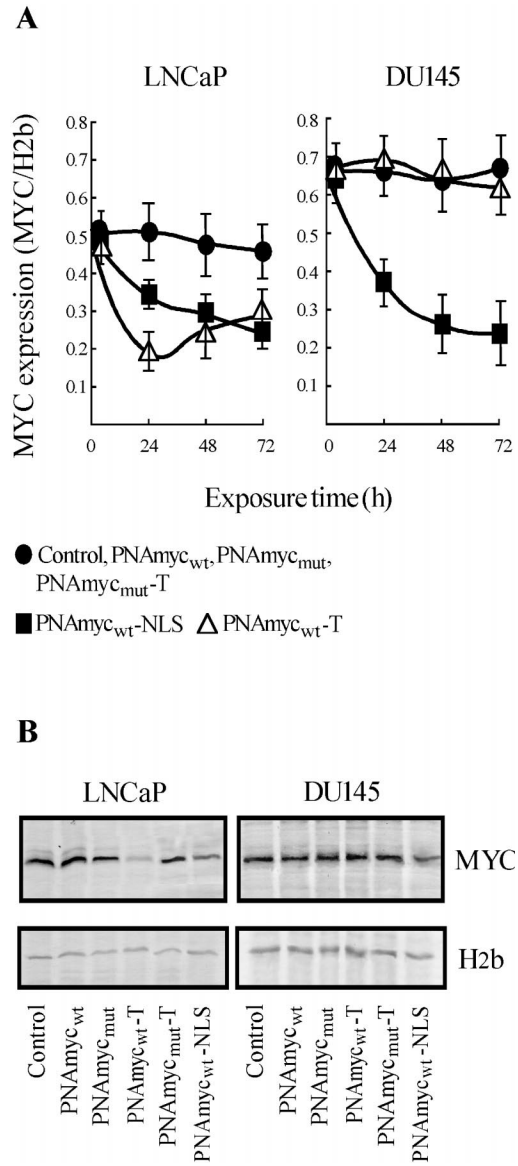

Fig. 4. Effect of the different specific PNA constructs on c-*myc* expression. LNCaP and DU145 cells were treated for the indicated time periods with a 10-μM concentration of PNA-myc$_{wt}$-T (△), PNA-myc$_{wt}$, PNA-myc$_{mut}$, PNA-myc$_{mut}$-T (●), and PNA-myc$_{wt}$-NLS (■). *A*, the amount of MYC protein was evaluated by Western blot analysis of total nuclear proteins. The results were obtained using image analysis of Western blot band intensities for MYC and histone H2b in the same electrophoretic separation determined by reaction with the specific antibodies. Data are reported as a ratio of the intensity of MYC:H2b. The SDs are illustrated. *B*, the pictures of Western bands for MYC and H2b at the 24-h exposure time point are shown.

Downloaded from http://aacrjournals.org/cancerres/article-pdf/60/8/2258/2484015/ch0800002258.pdf by guest on 06 October 2024

dent linear inhibition of MYC, reaching about 65% at 72 h. These results are significant as illustrated by the error bars in Fig. 4, *A* and *B*. None of the other listed PNAs had a significant effect.

A similar selective trend of MYC down-regulation by PNA-myc_{wt}-T was observed in preliminary experiments using rhodaminated PNAs when comparing PNA-myc_{wt}-R and PNA-myc_{wt}-TR at a much lower concentration (2 μM) because of limited solubility of these R-PNA constructs (see "Materials and Methods"). In this case, MYC showed a small selective decrease only in LNCaP cells treated with PNA-myc_{wt}-TR (−20% at 24 h; −30% at 48 and 72 h; data not shown).

How Specific is PNA Targeting of the c-*myc* Gene? Of particular significance are the comparative results obtained with PNAs complementary to unique c-*myc* sequence to those in which that sequence had been altered by a three-point mutation that did not change the ratio of purine: pyrimidine. The significant inhibition of MYC expression by PNAs containing the wild-type sequence is contrasted with the negligible effects of the PNA mutants in both LNCaP and DU145 cells (Fig. 4).

DISCUSSION

In considering the efficient application of PNAs as anti-gene and antisense agents, it is apparent that the ability to target a particular cell type would be highly advantageous. The experiments described in this study, comparing two prostatic cancer cell lines differing in their expression of the AR gene, show that a T vector covalently linked to a PNA anti-*myc* gene can discriminate between those cell types based on the presence or absence of the AR receptor. Taken together, the ability of the PNA-vector complex to enter and to remain within the nucleus of the targeted cells at a concentration that allows inhibition of MYC expression suggests that this strategy may have much wider applications: using other cancer cell types and different nuclear receptors, as well as different PNA sequences targeted to particular genes. These present results are consistent with increasing evidence (7, 11, 13–15, 23) that PNAs can bind their complementary sequences in chromatin with high specificity, thereby effectively blocking transcription and translation. Our data suggest that anti-gene PNAs selectively bind and down-regulate the complementary sequences in the target gene when linked to specific hormonal vectors. These vectors appear to facilitate the uptake of PNA into the nucleus of living cells, which contain their cognate hormone receptor, findings suggestive of vector-enhanced nuclear translocation mediated by AR.

ACKNOWLEDGMENTS

We thank Prof. A. Alagòn for his permission to use the microscopy facilities; Drs. X. Alvarado and A. Olvera for their excellent technical support with confocal microscopy (Instituto de Biotecnologia, Universidad Nacional Autonoma de Mexico, Cuernavaca, Mexico); L. Mitchell for cell culture expertise; Drs. E. M. Carpaneto and M. Ulivi for image analysis and artwork; and J. Schweis for editorial assistance.

REFERENCES

1. Egholm, M., Buchardt, O., Nielsen, P. E., and Berg, R. H. Peptide nucleic acids (PNA). Oligonucleotide analogues with an achiral peptide backbone. J. Am. Chem. Soc., *114:* 1895–1897, 1992.
2. Nielsen, P. E., Egholm, M., Berg, R. H., and Buchardt, O. Sequence-selective recognition of DNA by strand displacement with a thymine-substituted polyamide. Science (Washington DC), *254:* 1497–1500, 1991.
3. Egholm, M., Buchardt, O., Christensen, L., Behrens, C., Freier, S., Driver, D. A., Berg, R. H., Kim, S. K., Norden, B., and Nielsen, P. E. PNA hybridizes to complementary oligonucleotides obeying the Watson-Crick hydrogen-bonding rules. Nature (Lond.), *365:* 566–568, 1993.
4. Almarsson, O., Bruice, T. C., Kerr, J., and Zuckermann, R. N. Molecular mechanics calculations of the structures of polyamide nucleic acid DNA duplexes and triple helical hybrids. Proc. Natl. Acad. Sci. USA, *90:* 7518–7522, 1993.
5. Tomac, S., Sarkar, M., Ratilainem, T., Wittung, P., Nielsen, P., Norden, B., and Graslund, A. Ionic effects on the stability and conformation of peptide nucleic acids (PNA) complexes. J. Am. Chem. Soc., *118:* 5544–5552, 1996.
6. Bentin, T., and Nielsen, P. E. Enhanced peptide nucleic acid binding to supercoiled DNA: possible implications for DNA "breathing" dynamics. Biochemistry, *35:* 8863–8869, 1996.
7. Boffa, L. C., Carpaneto, E. M., Mariani, M. R., Louissaint, M., and Allfrey, V. G. Contrasting effects of PNA invasion of the chimeric DMMYC gene on transcription of its myc and PVT domains. Oncol. Res., *9:* 41–51, 1997.
8. Boffa, L. C., Carpaneto, E. M., and Allfrey, V. G. Isolation of active genes containing CAG repeats by DNA strand invasion by a peptide nucleic acid. Proc. Natl. Acad. Sci. USA, *92:* 1901–1905, 1995.
9. Demidov, V. V., Potaman, V. N., Frank-Kamenetskii, M. D., Egholm, M. E., Buchardt, O., Sonnichsen, S. H., and Nielsen, P. E. Stability of peptide nucleic acids in human serum and cellular extracts. Biochem. Pharmacol., *48:* 1310–1313, 1994.
10. Boffa, L. C., Morris, P. L., Carpaneto, E. M., Louissaint, M., and Allfrey, V. G. Invasion of the CAG triplet repeats by a complementary peptide nucleic acid inhibits transcription of the androgen receptor and TATA-binding protein genes and correlates with refolding of an active nucleosome containing a unique AR gene sequence. J. Biol. Chem., *271:* 13228–13233, 1996.
11. Tyler, B. M., Jansen, K., McCormick, D. J., Douglas, C. L., Boules, M., Stewart, J. A., Zhao, L., Lacy, B., Cusack, B., Fauq, A., and Richelson, E. Peptide nucleic acids targeted to the neurotensin receptor and administered i.p. cross the blood-brain barrier and specifically reduce gene expression. Proc. Natl. Acad. Sci. USA, *96:* 7053–7058, 1999.
12. Gray, D. G, Basu, S., and Wickstrom, E. Transformed and immortalized cellular uptake of oligodeoxynucleoside phosphorotioathes, 3′alkylamino oligodeoxynucleotides,2′-*O*-methyl oligo-ribonucleotides, oligodeoxynucleosides methylphosphonates, and peptide nucleic acids. Biochem. Pharmacol., *53:* 1465–1476,1997.
13. Bonham, M. A., Brown, S., Boyd, A. L., Brown, P. H., Bruckenstein, D. A., Hanvey, J. C., Thomson, S. A., Pipe, A., Hassman, F., Bisi, J. E., Froehler, B. C., Matteucci, M. D., Wagner, R. W., Noble, S. A., and Babiss, L. E. An assessment of the antisense properties of RNase H-competent and steric-blocking oligomers. Nucleic Acids Res., *23:* 1197–1203, 1995.
14. Pooga, M., Soomets, U., Hallbrink, M., Valkna, A., Saar, K., Rezaei, K., Kahl, U., Hao, J. X., Xu, X. J., Hallin, Z. W., Hokfelt, T., Bartfai, T., and Langel, U. Cell penetrating PNA constructs regulate galanin receptor levels and modify pain transmission *in vivo*. Nat. Biotechnol., *16:* 857–861, 1998.
15. Aldrian-Herrada, G., Desarmenien, M. G., Orcel, H., Boissin-Agasse, L., Mery, J., Brugidou, J., and Rabie, A. A peptide nucleic acid (PNA) is more rapidly internalized in cultured neurons when coupled to a retro-inverso delivery peptide. The antisense activity depresses the target mRNA and protein in magnocellular oxytocin neurons. Nucleic Acids Res., *26:* 4910–4916, 1998.
16. Scarfì, S., Gasparini, A., Damonte, G., and Benatti, U. Synthesis, uptake, and intracellular metabolism of a hydrophobic tetrapeptide-peptide nucleic acid (PNA)-biotin molecule. Biochem. Biophys. Res. Commun., *236:* 323–326, 1997.
17. Branden, L. J., Mohamed, A. J., and Edward Smith, C. I A peptide nucleic acid nuclear localization signal fusion that mediates nuclear transport of DNA. Nat. Biotechnol., *17:* 784–787, 1999.
18. Tilley, W. D., Wilson, C. M., Marcelli, M., and McPhaul, M. J. Androgen Receptor gene expression in human prostate carcinoma cell lines. Cancer Res., *50:* 5382–5386, 1990.
19. Trapman, J., and Brinkmann, A. O. The androgen receptor in prostate cancer. Pathol. Res. Pract., *192:* 752–760, 1996.
20. Balaji, K. C., Koul, H., Mitra, S., Maramag, C., Reddy, P., Menon, M., Malhotra, R. K., and Laxmanan, S. Antiproliferative effects of c-myc antisense oligonucleotide in prostate cancer cells: a novel therapy in prostate cancer. Urology, *50:* 1007–1015, 1997.
21. Grazin, C., Dupont de Dinechin, S., Hampe, S., Masson, J. M., Martin, P., Stehelin, D., and Galibert, F. Nucleotide sequence of the human c-myc locus: provocative open reading frame within the first exon. EMBO J., *3:* 383–387, 1984.
22. Lanford, R. E., Kanda, P., and Kennedy, R. C. Induction of nuclear transport with a synthetic peptide homologous to the SV40 T antigen transport signal. Cell, *46:* 575–582, 1986.
23. Cutrona, G., Carpaneto, E. M., Ulivi, M., Roncella, S., Landt, O., Ferrarini, M., and Boffa, L. C. Effects in live cells of a c-myc anti-gene PNA linked to a nuclear localization signal. Nat. Biotechnol., *18:* 300–303, 2000.
24. Merrifield, B. Concept and early development of solid-phase peptide synthesis. Methods Enzymol., *289:* 3–13, 1997.
25. Christensen, L., Fitzpatrick, R., Gildea, B., Petersen, K. H., Hansen, H. F., Koch, T., Egholm, M., Buchardt, O., Nielsen, P. E., Coull, J., and Berg, R. H. Solid-phase synthesis of peptide nucleic acids. J. Pept. Sci., *3:* 175–183, 1995.
26. Horoszewicz, J. S, Leong, S. S., Kawinski, E., Karr, J. P., Rosenthal, H., Chu, T. M., Mirand, E. A., and Murphy, G. P. LNCaP model of human prostatic carcinoma. Cancer Res., *43:* 1809–1818, 1983.
27. Mickey, D. D., Stone, K. R., Wunderli, H., Mickey, G. H., Vollmer, R. T., and Paulson, D. F. Heterotransplantation of a human prostatic adenocarcinoma cell line in nude mice. Cancer Res., *37:* 4049–4058, 1977.
28. Curtis Bird, R., Su, S., and Wu, G. J. E. Celis (ed.). Cell Biology: A Laboratory Handbook, Vol. 1, pp. 278. New York: Academic Press, 1994.
29. Cutrona, G., Ulivi, M., Fais, F., Roncella, S., and Ferrarini, M. Transfection of the c-myc oncogene into normal Epstein-Barr virus-harboring B cells results in new phenotypic and functional features resembling those of Burkitt Lymphoma cells and normal centroblasts. J. Exp. Med., *181:* 699–711, 1995.

Downloaded from http://aacrjournals.org/cancerres/article-pdf/60/8/2258/2484015/ch0800002258.pdf by guest on 06 October 2024